https://dx.doi.org/10.1016/j.bbrc.2020.07.050 This is the Preprint Version.

Schwann cell-specific *Pten* inactivation reveals essential role of the sympathetic nervous system activity in adipose tissue development

Xiao-Xiao Li[1, 4], Shi-Jie Zhang[1, 2, 4], Ka-Yi Man[1], Amy P. Chiu[1], Lilian H. Lo[1], Jeffrey C. To[1], Cynthia H. Chiu[1], Chi-On Chan[1], Daniel K.W. Mok[1], Dewi K. Rowlands[3], Vincent W. Keng[1,*]

[1]State Key Laboratory of Chemical Biology and Drug Discovery, Department of Applied Biology and Chemical Technology, The Hong Kong Polytechnic University, Hung Hom, Kowloon, Hong Kong SAR.

[2]Department of Neurology, The Second Affiliated Hospital of Guangzhou University of Chinese Medicine, Guangzhou, China.

[3]Laboratory Animal Services Centre, The Chinese University of Hong Kong, Sha Tin, New Territories, Hong Kong SAR.

[4]These authors contributed equally.

[*]Corresponding author

Vincent W. Keng

State Key Laboratory of Chemical Biology and Drug Discovery, Department of Applied Biology and Chemical Technology, The Hong Kong Polytechnic University, Hung Hom, Kowloon, Hong Kong SAR.

Email: vincent.keng@polyu.edu.hk

Telephone: +852-3400-8728

Fax: +852-2364-9932

Abstract

There is increasing evidence that the sympathetic nervous system (SNS) plays an important role in adipose tissue development. However, the underlying molecular mechanism(s) associated with this remains unclear. SNS innervation of white adipose tissue (WAT) is believed to be necessary and sufficient to elicit WAT lipolysis. In this current study, mice with Schwann cell (SC)-specific inactivation of *phosphatase and tensin homolog* (*Pten*) displayed enlarged inguinal white adipose tissue (iWAT). This serendipitous observation implicates the role of SCs in mediating SNS activity associated with mouse adipose tissue development. Mice with SC-specific *Pten* inactivation displayed enlarged iWAT. Interestingly, the SNS activity in iWAT of SC-specific *Pten*-deficient mice was reduced as demonstrated by decreased tyrosine hydroxylase (TH) expression level and neurotransmitters, such as norepinephrine (NE) and histamine (H). The lipolysis related protein, phosphorylated hormone sensitive lipase (pHSL), was also decreased. As expected, AKT-associated signaling pathway was hyperactivated and hypothesized to induce enlarged iWAT in SC-specific *Pten*-deficient mice. Moreover, preliminary experiments using AKT inhibitor AZD5363 treatment ameliorated the enlarged iWAT condition in SC-specific *Pten*-deficient mice. Taken together, SCs play an essential role in the regulation of SNS activity in iWAT development via the AKT signaling pathway. This novel role of SCs in SNS function allows for better understanding into the genetic mechanisms of peripheral neuropathy associated obesity.

Key words

Sympathetic nervous system; Schwann cell; white adipose tissue; Pten

Introduction

The worldwide incidence of being overweight, resulting in obesity, has doubled since 1980 to constitute nearly 30% of the world's population [1]. Currently, obesity has become one of the most common serious health problems. Accumulating studies have focused on revealing regulation of adipose tissue development, lipolysis and obesity-related diseases, such as type II diabetes and cardiovascular diseases. In this study, the role of Schwann cells (SCs) in regulating sympathetic nervous system (SNS) activity in white adipose tissue (WAT) regulation was investigated.

Energy is stored as triglycerides in WAT and this lipid storage can be mobilized via lipolysis by hydrolysis of triglycerides into glycerol and free fatty acids during energy shortage. Innervation of WAT by the SNS has been previously demonstrated and its activation is necessary for initiating lipolysis [2-4]. In addition, sympathetic nerve arborizations cover more than 90% of adipocytes in inguinal white adipose tissue (iWAT), indicating close anatomical and functional interactions [3,5]. Electrical or optogenetic stimulation of SNSs activity have been shown to induce lipolytic effects in WAT, while ablation of SNS inputs blocks this effects [6,7]. The catecholamines norepinephrine (NE), the principal neurotransmitter released by sympathetic nerves can activate lipolysis via the β3-adrenergic receptor (β3-AR) in rodents and β1, β2 receptors in humans [8,9], initiating the canonical intracellular events that activates hormone sensitive lipase (HSL) and perilipin A phosphorylation [10,11]. HSL catalyzes the conversion of diacylglycerol, the products of basal lipolysis produced by triglyceride lipase, into monoacyl-glycerol, which could serve as intracellular marker for SNS/NE induced lipolysis [2,4,12,13].

SCs are the major glia of the peripheral nervous system (PNS) and have many important functions. In the SNS, there are two types of neurons contributing to electrical signal transmission: preganglionic fibers that are wrapped by myelinated SCs and postganglionic

fibers that are wrapped by nonmyelinated SCs. SCs also promote nerve regeneration and reinnervation, indicating their importance in peripheral nerve repair [14-16]. However, it is challenging to obtain adequate amounts of autologous SCs from integrated nerves for research. Instead, SC-like cells from adipose-derived stem and bone marrow cells have become alternative sources [17-19]. More recently, SC-like cells have been isolated directly from murine iWAT [20]. This idea was derived from an observation that patients who undergo liposuction usually experience nerve injury but were then subsequently regenerated and repaired. However, the roles of SCs in adipose tissue lipid metabolism remain to be elucidated. In this current study, mice with SC-specific inactivation of *Pten* developed enlarged iWAT, indicating SCs may play an important role in adipose tissue metabolism.

While recent studies have demonstrated dense innervation of WAT by the SNS, the roles of SCs in SNS innervated WAT remain unclear. Our observation showed that SC-specific *Pten* inactivation induced activated AKT signaling pathway, resulting in enlarged iWAT, decreased SNS activity and reduced release of neurotransmitters. This phenotype associated with activated AKT signaling pathway was ameliorated when *Pten*-deficient mice were treated with the AKT inhibitor AZD5363. Taken together, SCs play an essential role in the regulation of SNS innervation of iWAT via the AKT signaling pathway.

Material and methods

Mouse breeding strategy and AZD5363 treatment

To obtain experimental mice with SC-specific of *Pten* gene, transgenic mice with *Pten* floxed exons 4 and 5 (encoding the phosphatase domain) were crossed to mice that express the Cre recombinase under the control of desert hedgehog *(Dhh)* regulatory elements for the generation of *Dhh*-Cre; $Pten^{flox/+}$ (*Dhh*-Cre; $Pten^{f/+}$). These mice were intercrossed to generate *Dhh*-Cre; $Pten^{flox/flox}$ (*Dhh*-Cre; $Pten^{f/f}$) experimental mice. All mice were PCR genotyped as previously described [21,22]. *Pten*-deficient mice were born at the expected mendelian frequency from the heterozygous intercross. The AKT inhibitor AZD5363 (MedChemExpress, New Jersey, USA) was first dissolved in DMSO at a stock concentration of 100 mg/ml. *Dhh*-Cre; $Pten^{f/f}$ mice were intraperitoneally injected with the AKT inhibitor AZD5363 at a dose of 20 mg/kg/day from postnatal day (P) 5 to P30. Mice were housed in a 12-hour light/dark cycle room with controlled temperature and humidity, with water and standard mouse chow *ad libitum*. All animal studies were approved by the appropriate ethics committee and performed in accordance with the ethical standards stipulated by both The Hong Kong Polytechnic University and The Chinese University of Hong Kong.

Fat index calculation

Fat index were determined using the following formula: fat tissue weight (g)/body weight (g) X 100.

Hematoxylin-eosin (HE) and immunohistochemical (IHC) staining

The iWAT fat tissues were freshly dissected and frozen in Tissue-Tek® OCT Compound (Sakura Finetek, California, USA) at -80°C overnight, followed by cryosectioning at 10 microns (Leica Biosystems, Wetzlar, Germany). Slides were stained with HE (Leica

Biosystems) using standard protocol. The IHC staining were performed as described previously [22]. The primary anti-tyrosine hydroxylase (TH) antibody (#AB152, Merck Millipore, Massachusetts, USA) was used at a dilution of 1:500.

Western blot analyses

Protein was isolated from iWAT and sciatic nerves of experimental mice using the Qproteome Mammalian Protein Prep Kit (Qiagen, Hilden, Germany) following the manufacturer's instructions. Protein concentration was determined using the Bradford Protein Assay (Bio-Rad Laboratories, California, USA). Protein were separated on an 8% SDS-PAGE gel and transferred to polyvinylidene difluoride (PVDF) membrane (Merck Millipore). Protein on the membrane were first incubated with indicated primary antibodies at 4°C overnight, followed by corresponding secondary antibody incubation at room temperature for 1.5 hours. Targeted proteins were detected using a horseradish peroxidase-conjugated chemiluminescent kit (Merck Millipore). Actin beta (ACTB) was used as the loading control. The antibodies used in this study were obtained from the following companies: phospho-AKT (#4060, Cell Signaling Technology, Massachusetts, USA), AKT (#4691, Cell Signaling Technology), HSL (#4107, Cell Signaling Technology), phospho-HSL (#4139, Cell Signaling Technology), TH (#AB152, Merck Millipore), and ACTB (#3700, Cell Signaling Technology). Semi-quantitative analyses of protein bands were measured using NIH ImageJ software. Intensity of bands was calculated as an arbitrary value relative to either the corresponding total protein or ACTB expression levels.

Neurotransmitter detection

The levels of norepinephrine, histamine and dopamine in iWAT were analyzed using Agilent 6460 liquid chromatography-triple quadrupole Mass Spectrometer (UPLC-QQQ-MS)

equipped with an electrospray ion source (The Hong Kong Polytechnic University, University Research Facility in Life Sciences). The columns used were ACQUITY BEH Amide columns (2.1 mm x 100 mm, 1.7 μm) and ACQUITY BEH Amide pre-columns (2.1 mm x 5 mm, 1.7 μm). Injection volume was 5 μl and sample chamber temperature was set at 4°C. The fragmentor voltages and collision energies were optimized for each neurotransmitter condition. Agilent MassHunter software version B.06.00 (quantitative data analysis) was used for data acquisition and processing.

Statistical analyses

Values are given as mean ± standard deviation (SD). Statistical significance was assessed by either two-tailed, unpaired Student's *t*-test or ordinary one-way ANOVA for multiple cohorts (Prism Software). *P* values < 0.05 were considered statistically significant.

Results

Conditional inactivation of Pten in SCs induced fat deposits in the lower belly

Representative transgene maps of *Dhh-Cre*, *Pten* wild type (WT), *Pten*$^{f/f}$ and *Dhh-Cre*; *Pten*$^{f/f}$ were shown in **Figure 1A**. A typical PCR genotyping result for *Dhh-Cre* and conditional *Pten* transgenes as illustrated (**Fig. 1B**). In *Dhh*-Cre; *Pten*$^{f/f}$ mice, increased size in the lower belly was consistently observed as a phenotype (*data not shown*). This phenomenon was caused by iWAT enlargement was observed during mouse necropsy at postnatal day 30 (P30) (**Fig. 1C**).

Conditional inactivation of Pten in SCs increased fat index and adipocyte size in iWAT

To determine whether the adipose tissue enlargement occurred in other adipose tissue types, the gonadal white adipose tissue (gWAT) and scapular brown adipose tissue (BAT) (representative of murine visceral WAT and BAT, respectively), were also collected for analyses (**Fig. 1C**). The fat index of iWAT was significantly increased in *Dhh*-Cre; *Pten*$^{f/f}$ mice (n = 7, 2.23 ± 0.16, mean ± SD) compared with that of control mice *Dhh*-Cre (n = 6, 0.60 ± 0.13) and *Dhh*-Cre; *Pten*$^{f/+}$ mice (n = 5, 0.75 ± 0.16) (**Fig. 1D**). However, fat index of iWAT in *Dhh*-Cre; *Pten*$^{f/+}$ mice showed no significant differences with that of control mice *Dhh*-Cre (P = 0.128, Student's t-test) (**Fig. 1D**). In addition, the gWAT and BAT fat indexes showed no statistical differences amongst all three experimental mouse cohorts using one-way ANOVA analyses (**Fig. 1D**). In order to confirm the morphological differences of the iWAT between control and *Pten*-deficient mice, HE staining was performed (**Fig. 1E**). The iWAT adipocytes from *Dhh*-Cre; *Pten*$^{f/f}$ mice were significantly larger in size compared with control mice (**Fig. 1E** and **1F**).

Upregulated AKT signaling pathway associated with inhibited SNS activity

Since PTEN is a known negative regulator of the PI3K/AKT pathway, the level of active phosphorylated AKT (pAKT) relative to total AKT in sciatic nerve lysate of *Dhh*-Cre; *Pten*$^{f/f}$ mice was investigated. As expected, significantly higher pAKT protein levels were detected in sciatic nerve lysate from *Dhh*-Cre; *Pten*$^{f/f}$ mice, compared with *Dhh*-Cre control group (**Fig. 2A**). Since SNS has been suggested to play an important role in WAT lipid metabolism, it was hypothesized that SC-specific *Pten* inactivation might also affect the SNS activity. Western blot and IHC analyses were used to determine tyrosine hydroxylase (TH) levels, a rate-limiting enzyme of catecholamine biosynthesis and a specific marker for sympathetic neurons. TH levels were significantly downregulated in iWAT of *Dhh*-Cre; *Pten*$^{f/f}$ mice compared with *Dhh*-Cre control mice by Western blot (**Fig. 2B**) and IHC analyses (**Fig. 2C**). These data suggest a novel interaction between SCs and AKT signaling pathway in SNS regulation of lipid metabolism.

Neurotransmitters norepinephrine (NE) and histamine (H) are used by the SNS to elicit lipolysis and accelerate its process in WAT, respectively. To further confirm that SNS activity was impaired in *Pten*-deficient mice, NE and H levels in iWAT were analyzed. NE and H levels were significantly reduced in iWAT of *Dhh*-Cre; *Pten*$^{f/f}$ mice compared with *Dhh*-Cre control mice (**Fig. 3A** and **3B**, respectively). Accordingly, dopamine (DA, direct precursor of NE) was also significantly decreased in *Dhh*-Cre; *Pten*$^{f/f}$ mice (**Fig. 3C**). As expected, the expression of phosphorylated hormone sensitive lipase (pHSL, downstream enzyme of norepinephrine-induced lipolysis) was also reduced in iWAT lysate of *Dhh*-Cre; *Pten*$^{f/f}$ mice compared with *Dhh*-Cre control mice (**Fig. 3D**).

AKT inhibitor AZD5363 improved SNS activity and reduced iWAT fat index

Upregulated pAKT levels and attenuated SNS activity were detected in iWAT lysate of *Dhh*-Cre; *Pten*$^{f/f}$ mice. In order to determine whether iWAT enlargement and SNS activity could

be ameliorated by targeting AKT signaling, *Dhh*-Cre; *Pten*$^{f/f}$ mice were treated with the AKT inhibitor AZD5363. The iWAT mass of AZD5363 treated mice were decreased compared with that of untreated mice (**Fig. 4A**). The iWAT fat index of AZD5363 treated mice were significantly reduced (P = 0.0184, Student's t-test), with the average of 1.88 ± 0.25, compared with the previous 2.23 ± 0.16 untreated group (**Fig. 4B**). However, iWAT fat index of AZD5363 treated mice were still significantly different from *Dhh*-Cre group (P < 0.0001, Student's t-test). Western blot was used to determine any improvement in SNS activity as a result of AZD5363 treatment (**Fig. 4C**). Relative expression levels of TH and total HSL levels in *Dhh*-Cre; *Pten*$^{f/f}$ iWAT were significantly increased (P < 0.05, Student's t-test) (**Fig. 4C**). However, there was no significant difference in relative pHSL to ACTB protein levels between DMSO and AZD5363 treated animals (P = 0.078, Student's t-test).

Discussion

The SNS has been previously shown to mobilize adipocytes through the neuro-adipose junctions in WAT, although the regulatory physiologic mechanisms responsible for this have not been fully determined. In this study, conditional inactivation of *Pten* gene specifically in SCs exhibited compromised SNS activity in WAT lipolysis, resulting in enlarged iWAT (**Fig. 1C** and **1D**). This suggests a novel interaction between SCs and AKT signaling pathway (**Fig. 2**) in SNS regulation of lipid metabolism (**Fig. 3**). Interestingly, treatment using the AKT inhibitor AZD5363 partly rescued this phenotype (**Fig. 4**). This data provides evidence on the essential regulatory role of SCs in mediating SNS activity in WAT development.

SNS innervation of WAT has been well studied, as well as its role in WAT lipid metabolism [4,23]. Given the anatomical relationship of SC in SNS, it is hypothesized that SCs could also contribute to essential SNS functions. The presence of SCs in WAT has been recently demonstrated by transmission electronic microscopy [20]. However, the role of SCs in WAT metabolic regulation remains to be elucidated, especially in the context of SNS functions. Most of the published works discussing the roles of SCs have focused on its function in PNS myelination process and its underlying mechanisms. SC-specific deletions of phosphatidylinositol 4-kinase alpha or fatty acid synthase have resulted in aberrant myelination [24,25]. AKT/mTOR pathway, *Big1*/*Arfgef1* and *Arf1*, as well as SC autophagy (myelinophagy) were proven to mediate myelination development in the PNS [26-29]. Neuregulin 1 regulate PNS myelination through activation of erythroblastic leukemia viral oncogene homolog-2/3 (ErbB2-3) receptor complexes in SCs [30]. Importantly, PTEN reduction in both oligodendrocytes and SCs induced hypermyelination while activated PTEN terminated myelination [31,32]. Taken together, SCs play a key role in the myelination process.

In the current study, mice with *Pten* mutation specifically in SCs displayed dysfunctional SNS activity, demonstrated by reduced TH expression and decreased release of neurotransmitters (NE, H and DA) in iWAT of *Dhh*-Cre; *Pten*$^{f/f}$ mice (**Fig. 3**). NE and H have been proven to be closely associated with SNS-driven lipolysis in WAT [33,34]. In addition, NE has been shown to inhibit adipocytes proliferation *in vitro* [35], which could have also contributed to iWAT enlargement in *Dhh*-Cre; *Pten*$^{f/f}$ mice (**Fig. 1C**). AKT inhibitor AZD5363 treatment partially rescued the iWAT phenotype in *Dhh*-Cre; *Pten*$^{f/f}$ mice, shown by decreased iWAT fat index. In addition, significantly elevated TH and HSL levels were identified in iWAT of AZD5363 treated *Dhh*-Cre; *Pten*$^{f/f}$ mice (**Fig. 4C**). Taken together, we conclude that functional SCs are important in regulating SNS functions in iWAT. In summary, the current study provides evidence that SCs play an essential role in mediating SNS functions in iWAT development via the AKT signaling pathway.

Acknowledgement

V.W.K. is supported by Collaborative Research Fund Equipment Grant (C5012-15E) and Research Impact Fund (R5050-18) from the Research Grant Council, Hong Kong Government; NSFC/RGC Joint Research Scheme (N-PolyU 503/16). State Key Laboratory of Chemical Biology and Drug Discovery, and Research Project Grants (ZE19, ZVLC, UA94, YBTA) funded by the Department of Applied and Chemical Technology, The Hong Kong Polytechnic University.

D.K.W.M. is supported by 153027/18P from the Research Grant Council of the Hong Kong Special Administrative Region; Hong Kong Chinese Materia Medica Standards Project, an internal grant (YBU0) and the Large Equipment Funds and University Research Facility in Chemical and Environmental Analysis of the Hong Kong Polytechnic University.

Reference

[1] Y.C. Chooi, C. Ding, F. Magkos, The epidemiology of obesity, Metabolism 92 (2019) 6-10.

[2] T.J. Bartness, Y. Liu, Y.B. Shrestha, V. Ryu, Neural innervation of white adipose tissue and the control of lipolysis, Frontiers in neuroendocrinology 35 (2014) 473-493.

[3] T.G. Youngstrom, T.J. Bartness, Catecholaminergic innervation of white adipose tissue in Siberian hamsters, American Journal of Physiology-Regulatory, Integrative and Comparative Physiology 268 (1995) R744-R751.

[4] T.J. Bartness, Y. Shrestha, C. Vaughan, G. Schwartz, C. Song, Sensory and sympathetic nervous system control of white adipose tissue lipolysis, Molecular and cellular endocrinology 318 (2010) 34-43.

[5] H. Jiang, X. Ding, Y. Cao, H. Wang, W. Zeng, Dense Intra-adipose Sympathetic Arborizations Are Essential for Cold-Induced Beiging of Mouse White Adipose Tissue, Cell metabolism 26 (2017) 686-692. e683.

[6] W. Zeng, R.M. Pirzgalska, M.M. Pereira, N. Kubasova, A. Barateiro, E. Seixas, Y.-H. Lu, A. Kozlova, H. Voss, G.G. Martins, Sympathetic neuro-adipose connections mediate leptin-driven lipolysis, Cell 163 (2015) 84-94.

[7] J.W. Correll, Adipose tissue: ability to respond to nerve stimulation in vitro, Science 140 (1963) 387-388.

[8] M. Lafontan, A. Bousquet‐Melou, J. Galitzky, P. Barbe, C. Carpéné, D. Langin, M. Berlan, P. Valet, I. Castan, A. Bouloumié, Adrenergic receptors and fat cells: differential recruitment by physiological amines and homologous regulation, Obesity 3 (1995).

[9] D. Langin, Adipose tissue lipolysis as a metabolic pathway to define pharmacological strategies against obesity and the metabolic syndrome, Pharmacological Research 53 (2006) 482-491.

[10] C. Holm, Molecular mechanisms regulating hormone-sensitive lipase and lipolysis, Portland Press Limited, 2003.

[11] W.-J. Shen, S. Patel, H. Miyoshi, A.S. Greenberg, F.B. Kraemer, Functional interaction of hormone-sensitive lipase and perilipin in lipolysis, Journal of lipid research 50 (2009) 2306-2313.

[12] A. Girousse, D. Langin, Adipocyte lipases and lipid droplet-associated proteins: insight from transgenic mouse models, International Journal of Obesity (2012) 581.

[13] D.L. Brasaemle, Thematic review series: adipocyte biology. The perilipin family of structural lipid droplet proteins: stabilization of lipid droplets and control of lipolysis, Journal of lipid research 48 (2007) 2547-2559.

[14] K.R. Jessen, R. Mirsky, A.C. Lloyd, Schwann cells: development and role in nerve repair, Cold Spring Harbor perspectives in biology 7 (2015) a020487.

[15] K. Jessen, R. Mirsky, The repair Schwann cell and its function in regenerating nerves, The Journal of physiology 594 (2016) 3521-3531.

[16] D.F. Kalbermatten, P. Erba, D. Mahay, M. Wiberg, G. Pierer, G. Terenghi, Schwann cell strip for peripheral nerve repair, Journal of Hand Surgery (European Volume) 33 (2008) 587-594.

[17] P.J. Kingham, D.F. Kalbermatten, D. Mahay, S.J. Armstrong, M. Wiberg, G. Terenghi, Adipose-derived stem cells differentiate into a Schwann cell phenotype and promote neurite outgrowth in vitro, Experimental neurology 207 (2007) 267-274.

[18] P. Lu, L. Jones, M. Tuszynski, BDNF-expressing marrow stromal cells support extensive axonal growth at sites of spinal cord injury, Experimental neurology 191 (2005) 344-360.

[19] M. Tohill, C. Mantovani, M. Wiberg, G. Terenghi, Rat bone marrow mesenchymal stem cells express glial markers and stimulate nerve regeneration, Neuroscience letters 362 (2004) 200-203.

[20] L. Chen, Y. Jin, X. Yang, Z. Liu, Y. Wang, G. Wang, Z. Qi, Z. Shen, Fat tissue, a potential Schwann cell reservoir: isolation and identification of adipose-derived Schwann cells, American journal of translational research 9 (2017) 2579.

[21] V.W. Keng, E.P. Rahrmann, A.L. Watson, B.R. Tschida, C.L. Moertel, W.J. Jessen, T.A. Rizvi, M.H. Collins, N. Ratner, D.A. Largaespada, PTEN and NF1 inactivation in Schwann cells produces a severe phenotype in the peripheral nervous system that promotes the development and malignant progression of peripheral nerve sheath tumors, Cancer research 72 (2012) 3405-3413.

[22] V.W. Keng, A.L. Watson, E.P. Rahrmann, H. Li, B.R. Tschida, B.S. Moriarity, K. Choi, T.A. Rizvi, M.H. Collins, M.R. Wallace, Conditional inactivation of Pten with EGFR overexpression in Schwann cells models sporadic MPNST, Sarcoma 2012 (2012).

[23] T. Bartness, V. Ryu, Neural control of white, beige and brown adipocytes, International journal of obesity supplements 5 (2015) S35.

[24] A. Alvarez-Prats, I. Bjelobaba, Z. Aldworth, T. Baba, D. Abebe, Y.J. Kim, S.S. Stojilkovic, M. Stopfer, T. Balla, Schwann-Cell-Specific Deletion of Phosphatidylinositol 4-Kinase Alpha Causes Aberrant Myelination, Cell reports 23 (2018) 2881-2890.

[25] L. Montani, J.A. Pereira, C. Norrmén, H.B. Pohl, E. Tinelli, M. Trötzmüller, G. Figlia, P. Dimas, B. von Niederhäusern, R. Schwager, De novo fatty acid synthesis by Schwann cells is essential for peripheral nervous system myelination, J Cell Biol 217 (2018) 1353-1368.

[26] E. Domènech-Estévez, H. Baloui, X. Meng, Y. Zhang, K. Deinhardt, J.L. Dupree, S. Einheber, R. Chrast, J.L. Salzer, Akt regulates axon wrapping and myelin sheath thickness in the PNS, Journal of Neuroscience 36 (2016) 4506-4521.

[27] Y. Miyamoto, T. Torii, K. Tago, A. Tanoue, S. Takashima, J. Yamauchi, BIG1/Arfgef1 and Arf1 regulate the initiation of myelination by Schwann cells in mice, Science advances 4 (2018) eaar4471.

[28] C. Norrmén, U. Suter, Akt/mTOR signalling in myelination, Portland Press Limited, 2013.

[29] J.A. Gomez-Sanchez, L. Carty, M. Iruarrizaga-Lejarreta, M. Palomo-Irigoyen, M. Varela-Rey, M. Griffith, J. Hantke, N. Macias-Camara, M. Azkargorta, I. Aurrekoetxea, Schwann cell autophagy, myelinophagy, initiates myelin clearance from injured nerves, J Cell Biol 210 (2015) 153-168.

[30] C. Birchmeier, K.A. Nave, Neuregulin‐1, a key axonal signal that drives Schwann cell growth and differentiation, Glia 56 (2008) 1491-1497.

[31] J.A. Pereira, F. Lebrun-Julien, U. Suter, Molecular mechanisms regulating myelination in the peripheral nervous system, Trends in neurosciences 35 (2012) 123-134.

[32] S. Goebbels, J.H. Oltrogge, R. Kemper, I. Heilmann, I. Bormuth, S. Wolfer, S.P. Wichert, W. Möbius, X. Liu, C. Lappe-Siefke, Elevated phosphatidylinositol 3, 4, 5-trisphosphate in glia triggers cell-autonomous membrane wrapping and myelination, Journal of Neuroscience 30 (2010) 8953-8964.

[33] H. Yoshimatsu, S. Hidaka, A. Niijima, T. Sakata, Histamine neurons down-regulate ob gene expression in rat white adipose tissue, Inflammation Research 50 (2001) 72-73.

[34] K. Tsuda, H. Yoshimatsu, A. Niijima, S. Chiba, T. Okeda, T. Sakata, Hypothalamic histamine neurons activate lipolysis in rat adipose tissue, Experimental biology and medicine 227 (2002) 208-213.

[35] T.J. Bartness, C.K. Song, H. Shi, R.R. Bowers, M.T. Foster, Brain–adipose tissue cross talk, Proceedings of the Nutrition society 64 (2005) 53-64.

Figure legends

Figure 1 Conditional inactivation of *Pten* in Schwann cells resulted in increased fat index and adipocyte size in iWAT. (**A**) Strategy for generating conditional inactivation of *Pten* specifically in Schwann cells. Representative transgene maps: top line shows the *Dhh*-Cre transgene; followed by *Pten* wild-type (WT) and floxed *Pten* allele ($Pten^{f/f}$), where loxP sites were indicated as black arrowheads. Finally, the mutant *Pten* allele in *Dhh*-Cre; $Pten^{f/f}$ mice after removal of exons 4 and 5 by Cre recombinase as shown in the last line. (**B**) A typical PCR genotyping result demonstrating the presence of *Dhh*-Cre transgene and various *Pten* floxed alleles. WT, wild-type adult mouse; DDW, water used as a negative control. (**C**) Representative images of iWAT, gWAT and BAT from three experimental mouse cohorts at postnatal 30-days. Scale bar, 1 cm. iWAT, inguinal white adipose tissue; gWAT, gonadal white adipose tissue; BAT, scapular brown adipose tissue. (**D**) Fat index of iWAT, gWAT and BAT from three experimental mouse cohorts. Values were expressed as mean ± SD; ****$P < 0.0001$ (Ordinary one-way ANOVA). (**E**) Representative HE staining images of iWAT from *Dhh*-Cre mouse and *Dhh*-Cre; $Pten^{f/f}$ mice. Scale bar, 100 μM. (**F**) Semi-quantification of adipocyte size (area per adipocyte) taken from multiple field of views from HE staining images. Values were expressed as mean ± SD; ****$P < 0.0001$ (Student's *t*-test).

Figure 2 Activated AKT signaling and compromised SNS activity in *Dhh*-Cre; $Pten^{f/f}$ mice. (**A**) Representative Western blot and semi-quantitative analyses of AKT signaling expression in sciatic nerves of experimental mice. pAKT, phospho-AKT; AKT, total AKT; ATCB, actin beta used as loading control. Relative pAKT to total AKT protein levels expressed as mean ± SD; ***$P = 0.003$ (Student's *t*-test). (**B**) Representative Western blot and semi-quantitative analyses demonstrating compromised SNS activity by reduced TH expression in iWAT of experimental mice. TH, tyrosine hydroxylase. Relative TH to ACTB

protein levels expressed as mean ± SD; *$P < 0.05$ (Student's *t*-test). (**C**) Representative IHC analyses showing reduced TH expression in iWAT of *Dhh*-Cre; *Pten*$^{f/f}$ mice. Scale bar, 100 μM.

Figure 3 Reduced neurotransmitter content in iWAT of *Dhh*-Cre; *Pten*$^{f/f}$ mice. (**A, B** and **C**) Norepinephrine (NE), histamine (H) and dopamine (DA) levels were analyzed in iWAT of *Dhh*-Cre and *Dhh*-Cre; *Pten*$^{f/f}$ mice using UPLC-QQQ-MS detection method, respectively. Values expressed as mean ± SD; ***$P = 0.0001$, **$P < 0.02$, *$P < 0.05$ (Student's *t*-test). (**D**) Representative Western blot and semi-quantitative analyses showing compromised lipolysis in iWAT of *Dhh*-Cre; *Pten*$^{f/f}$ mice. pHSL, phosphorylated hormone sensitive lipase; HSL, total hormone sensitive lipase. Relative pHSL to total HSL protein levels expressed as mean ± SD; **$P < 0.005$ (Student's *t*-test).

Figure 4 AKT inhibitor AZD5363 improved SNS activity and reduced iWAT fat index in *Dhh*-Cre; *Pten*$^{f/f}$ mice. *Dhh*-Cre; *Pten*$^{f/f}$ mice were treated with either 20 mg/kg/day AKT inhibitor AZD5363 from P5 to P30. (**A**) Representative images of iWAT from untreated and AKT inhibitor (AZD5363) treated groups. Scale bars, 1 cm. (**B**) Fat index of iWAT from untreated and AZD5363 treated groups. Values expressed as mean ± SD; *$P = 0.0184$ (Student's *t*-test). (**C**) Representative Western blot and semi-quantitative analyses showing improved TH expression and increased total HSL in treated animals. TH, tyrosine hydroxylase; HSL, total hormone sensitive lipase. Values expressed as mean ± SD; *$P < 0.05$ (Student's *t*-test).

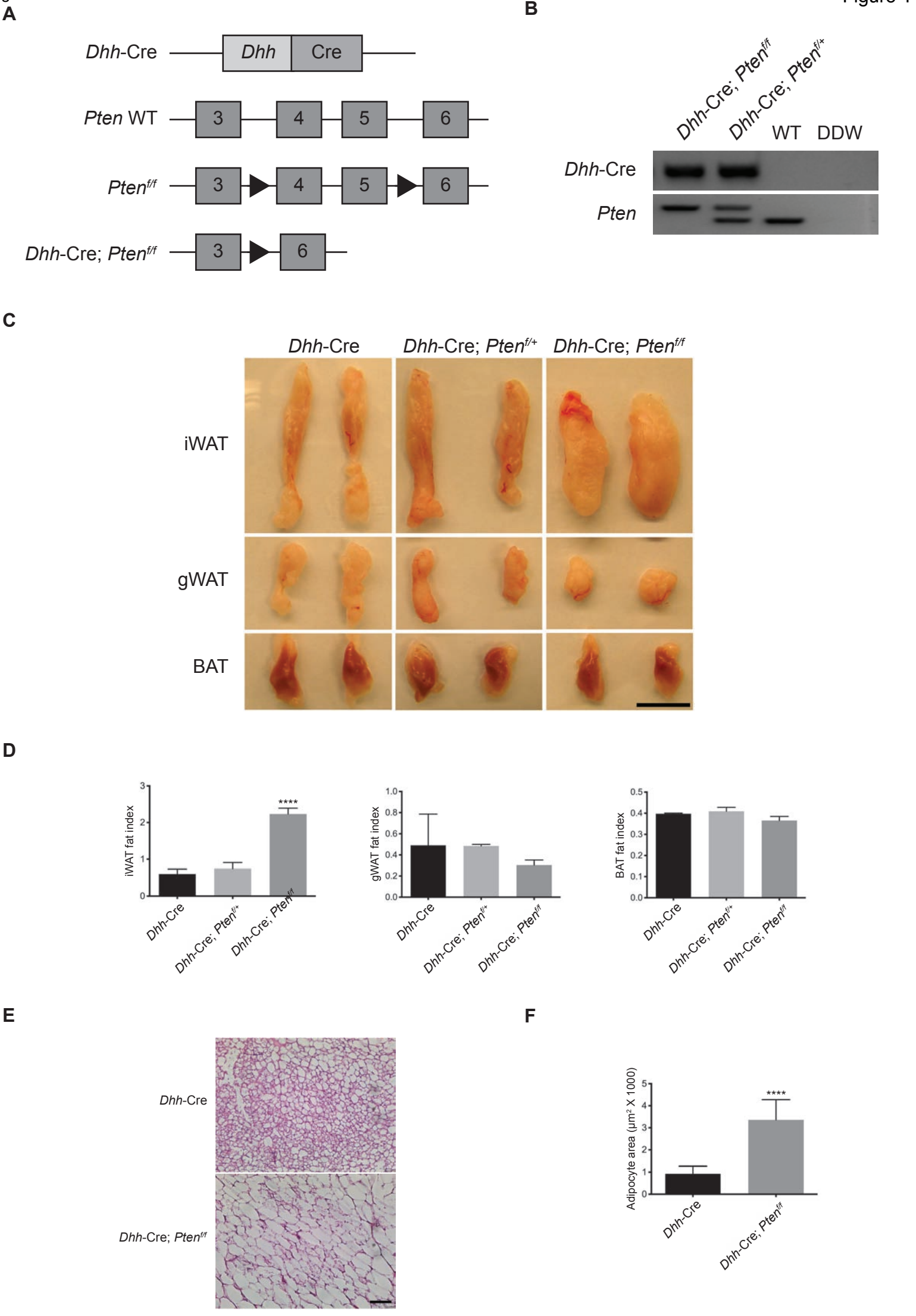
A
Dhh-Cre
Dhh
Cre
Pten WT
3
4
5
6
Pten f/f
Dhh-Cre; Pten f/f
B
Dhh-Cre; Pten f/f
Dhh-Cre; Pten f/+
WT
DDW
Dhh-Cre
Pten
C
Dhh-Cre
Dhh-Cre; Pten f/+
Dhh-Cre; Pten f/f
iWAT
gWAT
BAT
D
iWAT fat index
****
gWAT fat index
BAT fat index
Dhh-Cre
Dhh-Cre; Pten f/+
Dhh-Cre; Pten f/f
E
Dhh-Cre
Dhh-Cre; Pten f/f
F
Adipocyte area (μm² X 1000)
****
Dhh-Cre
Dhh-Cre; Pten f/f

A

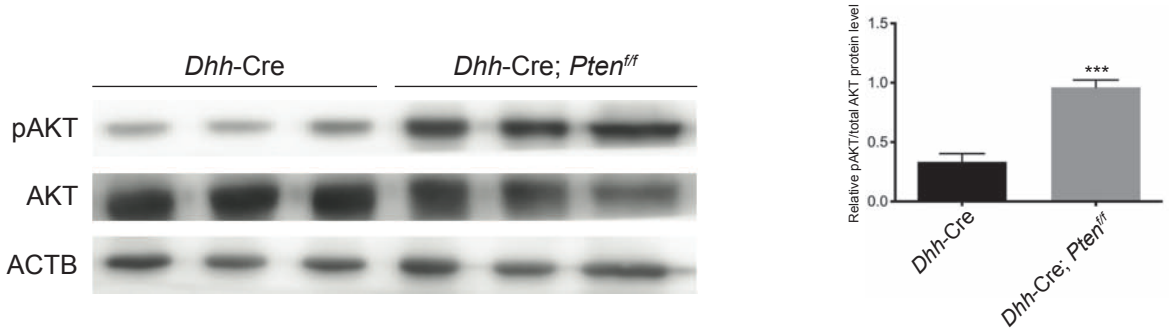
Dhh-Cre
Dhh-Cre; Pten f/f
pAKT
AKT
ACTB
Relative pAKT/total AKT protein level
1.5
1.0
0.5
0.0
***
Dhh-Cre
Dhh-Cre; Pten f/f

B

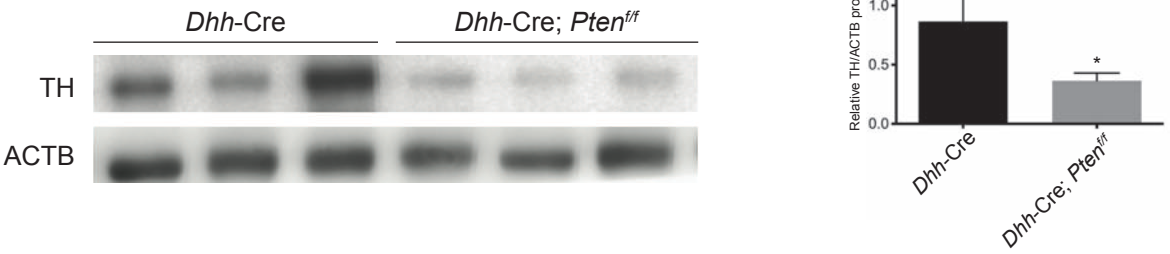
Dhh-Cre
Dhh-Cre; Pten f/f
TH
ACTB
Relative TH/ACTB protein level
1.5
1.0
0.5
0.0
*
Dhh-Cre
Dhh-Cre; Pten f/f

C

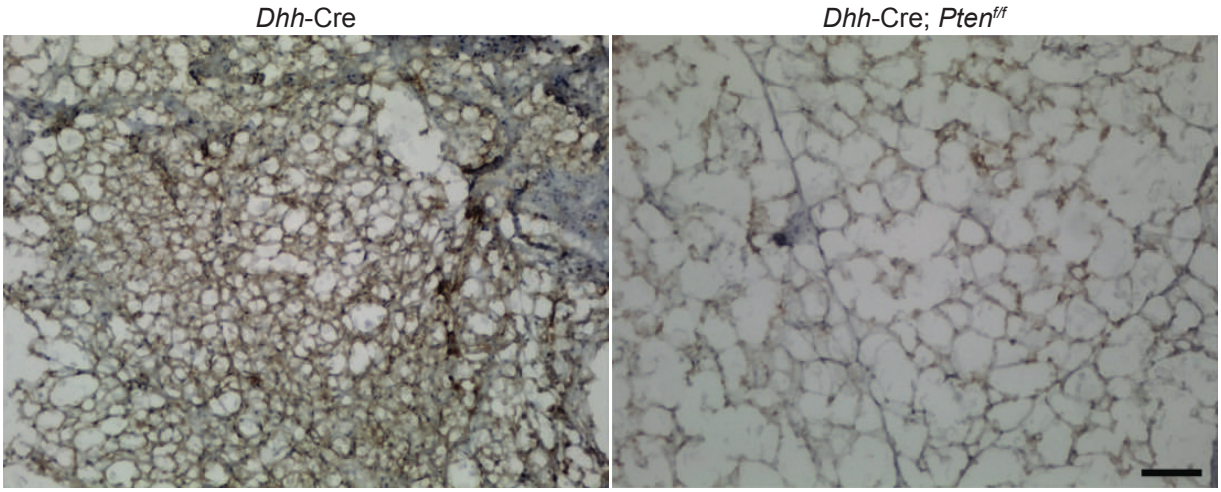
Dhh-Cre
Dhh-Cre; Pten f/f

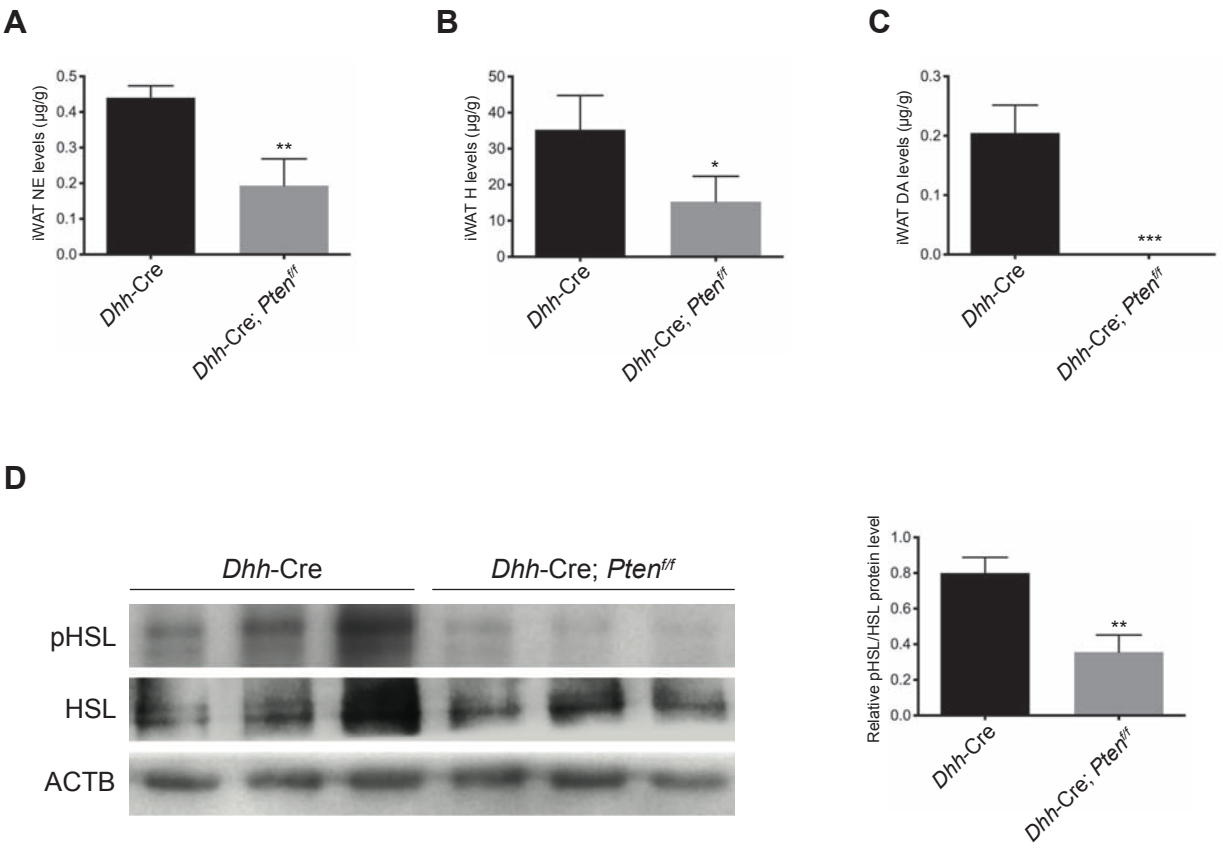
A
iWAT NE levels (μg/g)
0.5
0.4
0.3
0.2
0.1
0.0
**
Dhh-Cre
Dhh-Cre; Pten f/f
B
iWAT H levels (μg/g)
50
40
30
20
10
0
*
Dhh-Cre
Dhh-Cre; Pten f/f
C
iWAT DA levels (μg/g)
0.3
0.2
0.1
0.0
***
Dhh-Cre
Dhh-Cre; Pten f/f
D
Dhh-Cre
Dhh-Cre; Pten f/f
pHSL
HSL
ACTB
Relative pHSL/HSL protein level
1.0
0.8
0.6
0.4
0.2
0.0
**
Dhh-Cre
Dhh-Cre; Pten f/f

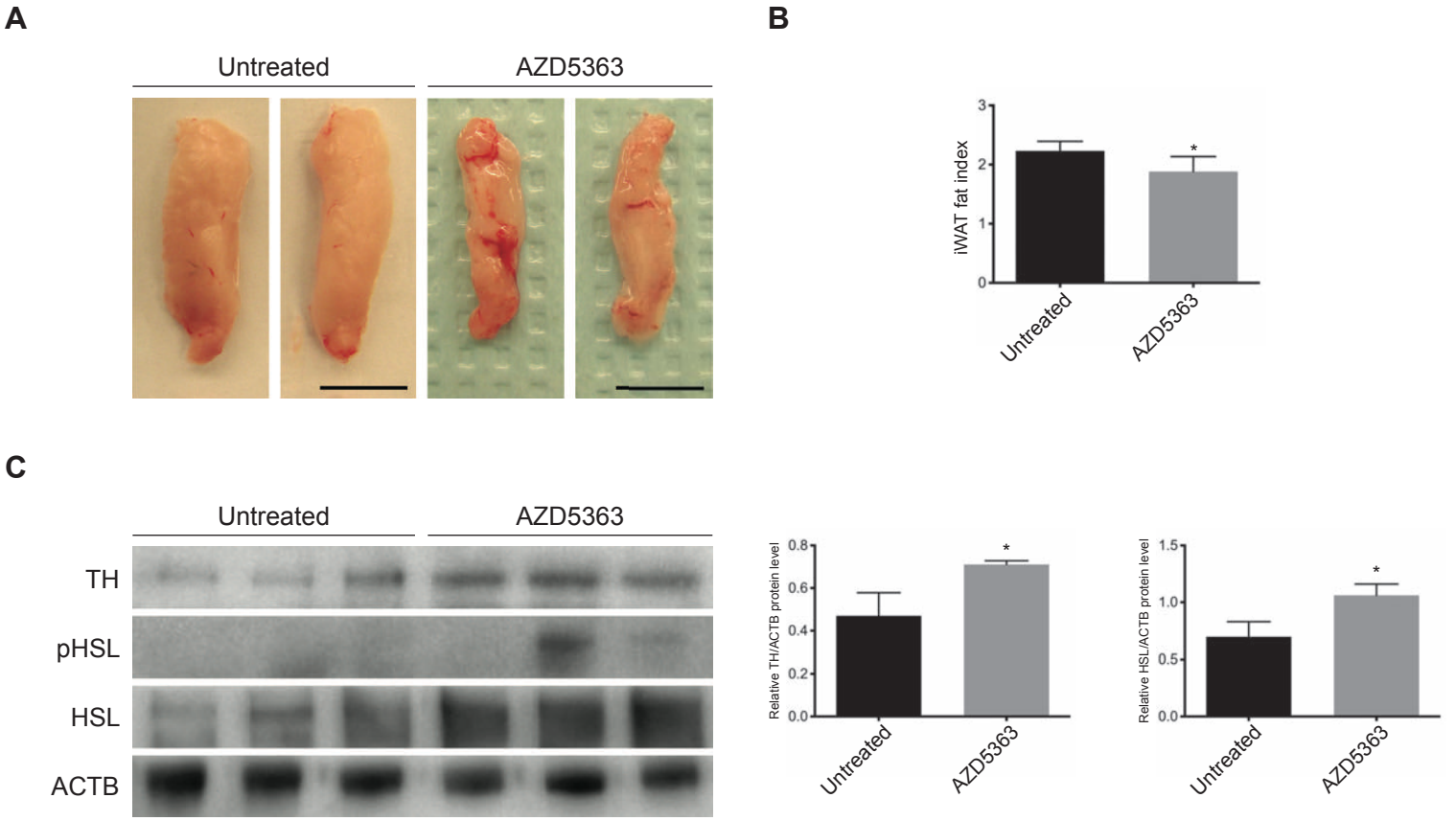
A
Untreated
AZD5363
B
iWAT fat index
3
2
1
0
*
Untreated
AZD5363
C
Untreated
AZD5363
TH
pHSL
HSL
ACTB
Relative TH/ACTB protein level
0.8
0.6
0.4
0.2
0.0
*
Untreated
AZD5363
Relative HSL/ACTB protein level
1.5
1.0
0.5
0.0
*
Untreated
AZD5363